A Novel Self-Consistent Model Based Optimal Filter Design for the Improved Dynamic Performance of 3-phase PLLs for Phase Tracking Under Grid Imperfections

Sambhav R Jain, Pradhyumna Ravikirthi & Nagamani Chilakapati

Journal of Control, Automation and Electrical Systems
formerly CONTROLE & AUTOMAÇÃO

ISSN 2195-3880
Volume 25
Number 5

J Control Autom Electr Syst (2014)
25:620-628
DOI 10.1007/s40313-014-0136-4

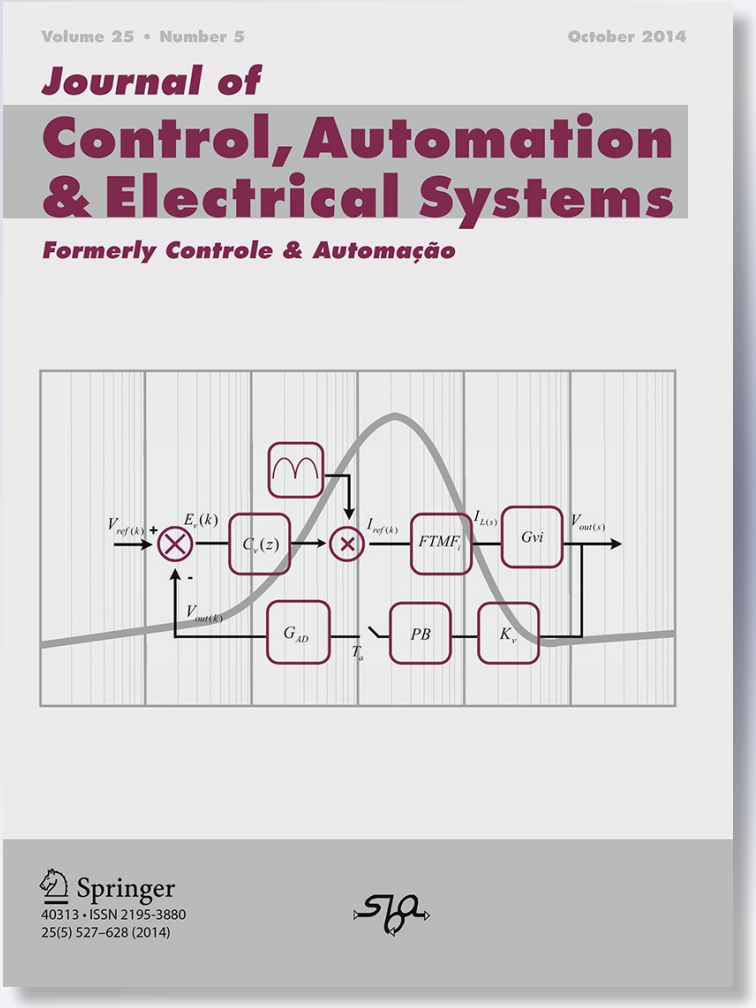

Springer

J Control Autom Electr Syst (2014) 25:620–628
DOI 10.1007/s40313-014-0136-4

A Novel Self-Consistent Model Based Optimal Filter Design for the Improved Dynamic Performance of 3-phase PLLs for Phase Tracking Under Grid Imperfections

Part 2: Analysis and Verification

Sambhav R Jain · Pradhyumna Ravikirthi · Nagamani Chilakapati

Received: 21 October 2013 / Revised: 23 March 2014 / Accepted: 13 May 2014 / Published online: 4 June 2014

Abstract In the context of recent advancements in 3-phase phase-locked loop (PLL) structures to tackle grid imperfections, this paper attempts to shift focus towards dynamic response optimization for fast tracking of disturbed grids, as opposed to Wiener optimization, a *trade-off* between filtering characteristic and dynamic response. In this respect, an ingenious self-consistent model (SCM) based approach is proposed which explores filter design in the presence of frequency shifts and phase jumps, and facilitates the analytical computation of *unique* loop filter parameters. Trial and error in filter parameter selection is inconvenient, but more importantly, even rigorous trials would be insufficient in qualifying the non-existence of a better design. Having eliminated trial and error, this novel technique limits transients to user specifications while fixing on an optimum damping ratio, to yield the best fit. The design methodology is applied to three existing 3-phase PLL structures modelled in MATLAB/Simulink, and the proposed method is further evaluated through extensive simulations and performance comparisons with the traditional Wiener approach. To enhance the understanding of model behaviour and the feasibility of practical implementation, comprehensive three-dimensional (3-D) lookup tables are presented. They enable the study of optimized filter parameter variations for a range of grid disturbances, and broaden the application to filter optimization in real-time. In the interest of the reader, this paper is structurally split in two parts. Part 1 covers the premise and theory that explicates the proposed SCM methodology. The detailed analysis and verification of the SCM is covered in Part 2.

Keywords Self-consistent model · Loop filter design · 3-D lookup tables · Dynamic performance · Wiener optimization · Grid imperfections

List of symbols

δ	Damping ratio
ω_n	Natural frequency (rad s^{-1})
k_p	Proportional gain of the PI controller
k_i	Integral gain of the PI controller
τ	Time constant of the designed filter (s)
$\Delta\omega_{\text{step}}$	Frequency step (Hz)
ϕ	Phase jump (rad)
E	Permissible phase error band (rad)
t_0	Settling time (s)

1 Brief Recapitulation of Literature

In Part 1 of this paper, we see the importance of the synchronous reference frame (SRF) PLL (Kaura and Blasko 1997; Chung 2000) in the context of grid synchronization, and its fundamental limitation in tracking a polluted grid (Karimi-Ghartemani and Iravani 2004; Silva et al. 2010). To overcome this, the SRF PLL has undergone several topological improvements as in the case of the dual second-order generalized integrator (DSOGI) PLL (Rodríguez et al. 2006), the decoupled double synchronous reference frame (DDSRF) PLL (Rodríguez et al. 2007), and the multiple complex coef-

S. R. Jain (✉) · P. Ravikirthi · N. Chilakapati
Department of Electrical and Electronics Engineering, National Institute of Technology, Tiruchirappalli 620015, India
e-mail: sambhav.eee@gmail.com

P. Ravikirthi
e-mail: pradhyumnarao@gmail.com

N. Chilakapati
e-mail: cnmani@nitt.edu

Present address:
S. R. Jain
Texas Instruments (India) Pvt. Ltd., Bagmane Tech Park, C V Raman Nagar, Bangalore 560093, India

ficient filter (MCCF) PLL (Guo et al. 2011). While these advanced PLLs address the filtering limitation of a stand-alone SRF PLL, they still rely on the Wiener optimization method (Gardner 2005) which uses a trade-off between filtering and fast tracking, in tuning the filter parameters. The poor dynamic response of SRF-based 3-phase PLLs is attributed to the PI based control (Silva et al. 2010; Liccardo et al. 2011; Lee et al. 2014). The need for better tuning of the PI filter parameters is also highlighted in Golestan et al. (2012); Kulkarni and John (2013). With this background, Part 1 presents the theory of the self-consistent model (SCM) based filter design, which not only focuses on dynamic performance optimization but also introduces a direct analytical method of fixing the controller gains.

2 Practical Realization Using 3-D Lookup Tables

From a designer's perspective, the SCM is convenient since by merely specifying the error limits at settling time, for a given maximum expected frequency excursion and phase jump in the grid voltage, the model generates a *unique parameter set* to quantize error with optimum dynamic performance and filter realizability.

It is noted that by definition, $\Delta\omega_{\text{step}}$ and ϕ are considered for the worst-case situation, and any other case will only be less stringent in terms of frequency excursion and/or phase jump. However, it would be useful to generate the unique parameter set for every possible combination of frequency step and phase jump in an acceptable range. For instance, the parameter set ($\{\delta, \omega_n, k_p, k_i, \tau\}$) can be calculated for $\Delta\omega_{\text{step}}$ in the range $[-20, 20]$ Hz and ϕ in the range $[-1, 1]$ rad. The number of data points in this range depends on the desired resolution (say increment of $\Delta\omega_{\text{step}}$ in 0.5 Hz and increment of ϕ in 0.025 rad). The resulting computation is done for $\frac{20-(-20)}{0.5} = 80$ values of $\Delta\omega_{\text{step}}$ and $\frac{1-(-1)}{0.025} = 80$ values of ϕ. i.e., the SCM is solved for $80 \times 80 = 6{,}400$ times. Hence, we get 6,400 optimum filter parameter sets which correspond to 6,400 unique values of $(\Delta\omega_{\text{step}}, \phi)$ in the specified range.

With $\Delta\omega_{\text{step}}$ defined along the x-axis and ϕ along the y-axis, each of the unique filter parameters is plotted along the z-axis, to obtain the 3-D lookup tables. Thus five lookup tables, computed for $E = 0.02$ rad, $t_0 = 0.01$ s, $\Delta\omega_{\text{step}} \in [-20, 20]$ Hz and $\phi \in [-1, 1]$ rad, were obtained as shown in Fig. 1. With the SCM implemented in MATLAB, the plots were generated from 6,400 iterations of this approach, under the run-time of a mere couple of minutes.

The 3-D lookup tables provide the following insights into the design intricacies of the loop filter parameters.

1. Symmetry about the origin: The nature of variation of the filter parameters in the 1st quadrant ($\Delta\omega_{\text{step}} = +\text{ve}$, $\phi = +\text{ve}$) is similar to that in the 3rd quadrant ($\Delta\omega_{\text{step}} = -\text{ve}$, $\phi = -\text{ve}$); same applies to the variation in the 2nd and 4th quadrant. This can also be corroborated from the sign of c_2, where $c_2 = \Delta\omega_{\text{step}}\phi\omega_n$ (see Part 1).
2. One can expect less strained parameters at lower values of $\Delta\omega_{\text{step}}$ and ϕ, through intuition. This is verified from the lookup tables.
3. From Fig. 1c and d, it can be inferred that the filter parameters are more stressed when $\Delta\omega_{\text{step}}$ and ϕ are of the opposite polarity (in 2nd and 4th quadrants) as compared to the case when both have the same polarity (in 1st and 3rd quadrants). Interestingly, from the error quantization equation (see Part 1), the error band E is always less when c_2 is positive, which is the case when both frequency excursion and phase jump are of the same polarity.
4. Filter realizability and speed of response: Time constant τ of the designed filter is an indication of the time margin the filter has, to respond to a stimulus and contain the error within the limits. It can be seen from Fig. 1e, that for smaller limits of $\Delta\omega_{\text{step}}$ and ϕ in the input, the filter has more time margin to contain the error, thus improving the ease of practical filter implementation as much as possible. The proposed scheme thereby does a best fit of the required dynamic performance with optimum filter realizability.

For implementation in real-time, the SCM may be solved once off-line for a worst-case range of $\Delta\omega_{\text{step}}$ and ϕ in the grid, and the optimized values of the loop filter parameters can be stored in the form of a lookup table on a microcontroller (or DSP). The lookup table can then be used to dynamically pick an optimized pair of (k_p, k_i) for a maxima of frequency excursion and a maxima of phase jump occurring in a certain period of time.[1] On a side note, the negative sign of controller gains in Fig. 1c and d is due to the convention of $E_m = -V_m$ adopted in the SRF PLL linear model (recall from Part 1). For interpretations, the absolute value of gains may be used.

3 Verification of the SCM Based Filter Design Through Simulations and Performance Comparisons

In this section, the SCM methodology is evaluated using comprehensive simulations, and the underlying theory is justified by making suitable comparisons with the traditional Wiener optimization method.

[1] Although the maxima would only indicate the magnitude of frequency step or phase jump, the filter needs to be designed with respect to the worst combination of the two, which is when both are of opposite polarities.

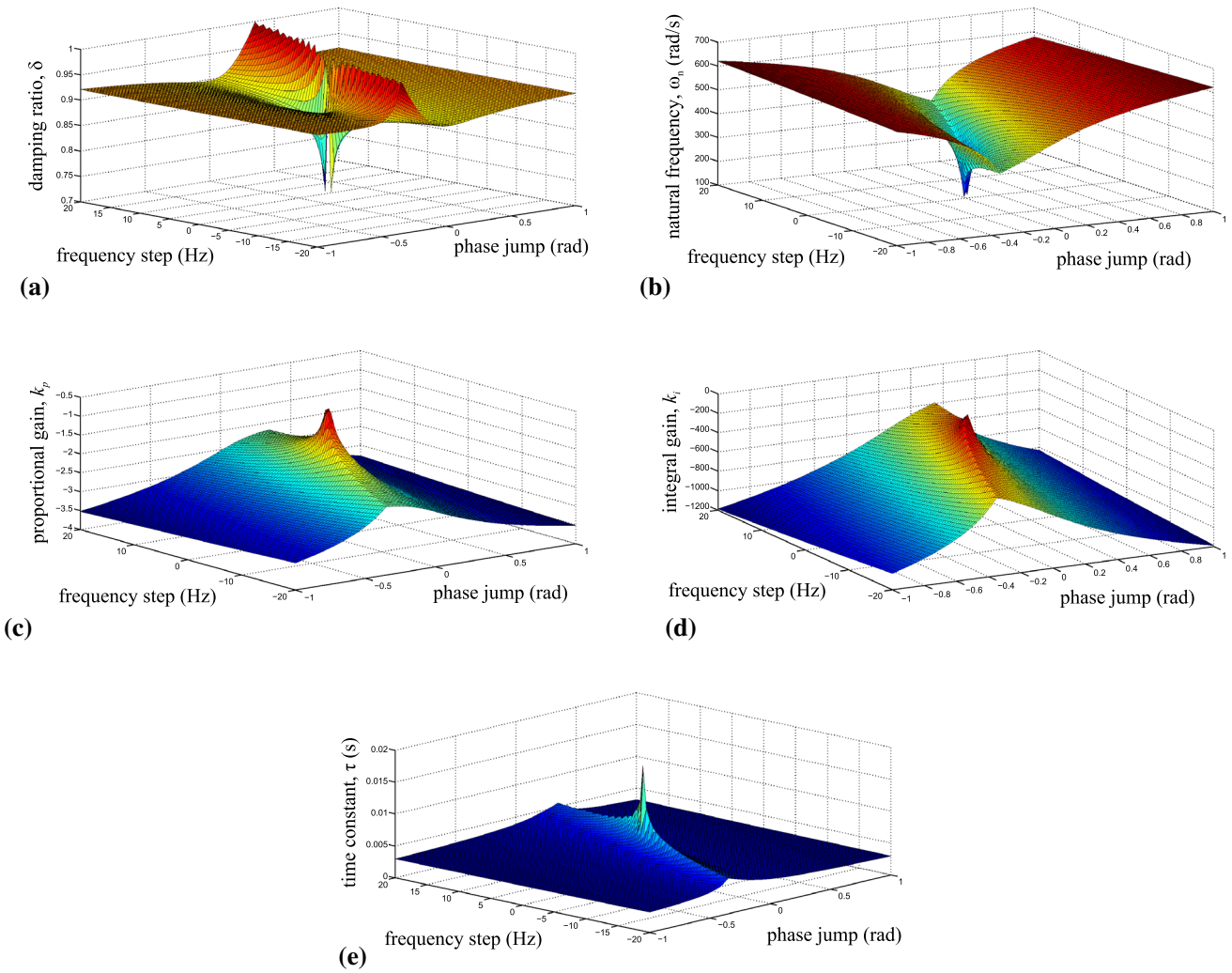

Fig. 1 3-D lookup tables for a range of frequency excursion and phase jump **a** Lookup table for the optimized value of damping ratio, **b** Lookup table for the optimized value of natural frequency, **c** Lookup table for the optimized value of proportional gain, **d** Lookup table for the optimized value of integral gain, **e** Lookup table for the optimized value of time constant (Color figure online)

Figure 2 shows the system under study comprising a 3-phase grid simulator which generates a 230 V, 50 Hz, 3-phase voltage under balanced conditions, and which can create frequency excursions and phase jumps of the desired magnitude. To simulate utility distortions, the grid simulator injects up to 10 % of unbalance and/or 5th, 7th, 11th and 13th order of harmonics in decreasing proportions. This grid voltage is then fed to a 3-phase PLL scheme. The outputs of the PLL, namely the space vector, voltage error, estimated frequency and phase are useful in deducing performance comparisons between the two methods of filter design.

Since the proposed approach is applicable to any improvised 3-phase PLL that uses SRF as the terminal stage, we have chosen three such PLLs from literature *viz.*, DDSRF, DSOGI, and MCCF PLL. These schemes are modelled in MATLAB/Simulink, and are subject to different grid imperfections. Parameters like phase tracking error, dynamic performance (in limiting error at settling time), ease of filter

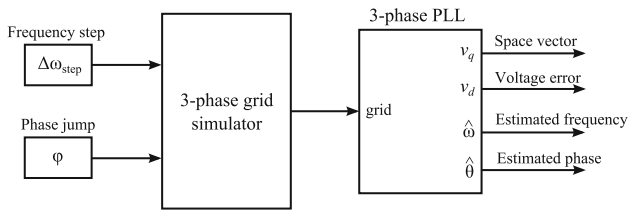

Fig. 2 System under study

parameter realization, and number of tuning iterations form the basis of comparison between the Wiener and the SCM methods of filter design.

3.1 Error Quantization Using the SCM

Consider a case where the specification is to limit the phase error band E within 0.02 rad at settling time $t_0 = 0.01$ s, for a worst-case phase jump of $\phi = \pi/6$ rad.

Table 1 Filter design using the Wiener and the proposed SCM method, for a maximum error band of 0.02 rad at settling time 0.01 s, when the SRF PLL is subject to a phase jump of $\pi/6$ rad

Method		δ	ω_n (rad s^{-1})	k_p	k_i	τ (ms)	Bandwidth $2\delta\omega_n$ (rad s^{-1})	Error band observed at t_0 (rad)
Wiener	Trial-1	0.707	314.16	−1.37	−303.4	4.50	444.2	0.160
	Trial-2		598.32	−2.60	−1100.6	2.36	846.0	0.022
	Trial-3	0.707	531.71	−2.31	−869.2	2.66	751.8	0.035
	Trial-4	0.96		−3.14	−869.2	3.61	1020.9	0.023
SCM		0.91	531.71	−2.97	−869.2	3.42	968.1	0.020

The Wiener approach involves fixing the value of one variable (δ), and tuning the other (ω_n), until a desired trade-off is obtained between filtering response and transient behaviour. In other words, the tuning here is limited to a small range of bandwidths, due to the inverse dependency discussed in Part 1. As it is seen, this method does not take into account the error limits and dynamic performance requirements in its computation, thereby inviting trial and error. To start with, the damping ratio is fixed at $\delta = 1/\sqrt{2}$ and the natural frequency is chosen as $\omega_n = 100\pi$ rad s^{-1}. When subject to a phase jump of $\pi/6$ rad, the instantaneous error in the tracked phase of the SRF PLL is 0.07958 rad (magnitude) at 0.01 s, while the error envelope spans to 0.16 rad, recorded under Trial-1 Wiener method in Table 1. Although the error band would eventually be contained to 0.02 rad due to the damped nature of oscillations, the designed loop filter shows inadequate dynamic performance as the error criterion is not met at the settling time specified.

On the other hand, the SCM uses the specified error, transient limits, worst-case frequency step and phase jump for which the system is to be designed, and computes a unique and optimized pair of design parameters (in this case, $\delta = 0.91$ and $\omega_n = 531.71$ rad s^{-1}). Since these values are computed by the self-consistent algorithm, no manual intervention is required in tuning them for further optimization. It will be shown that the computed values not only limit error at the settling time, but also do so with the optimum choice of filter parameters, to enhance ease of filter realizability on a practical setup.

The response of the SRF PLL when subject to a phase jump of $\pi/6$ rad is compared in Fig. 3, between the Trial-1 Wiener optimized values ($\delta = 0.707$, $\omega_n = 314.16$ rad s^{-1}), and the SCM computed values ($\delta = 0.91$, $\omega_n = 531.71$ rad s^{-1}). It is observed that the phase error settles to zero more quickly and has a smaller overshoot with the SCM filter design.

Figure 4 records the instantaneous error in the two cases to verify error quantization at settling time. The data-tip shows a phase error of 0.009795 rad (magnitude) at 0.01 s with the SCM method. Clearly, the error band at this instant is

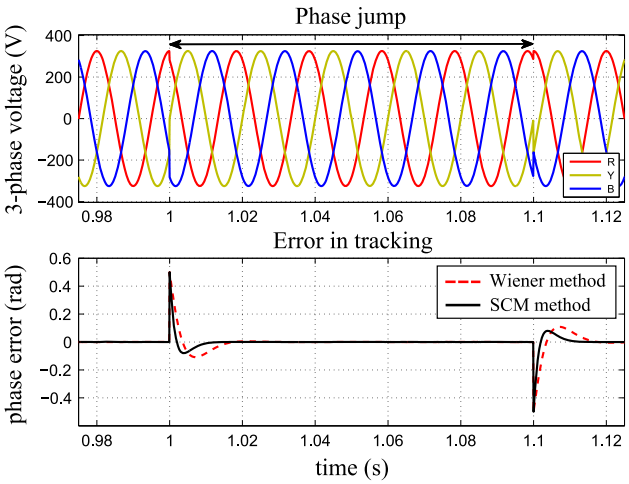

Fig. 3 Comparison of the phase error of SRF PLL when subject to a phase jump of $\pi/6$ rad, between the Wiener and the proposed SCM method of filter design (Color figure online)

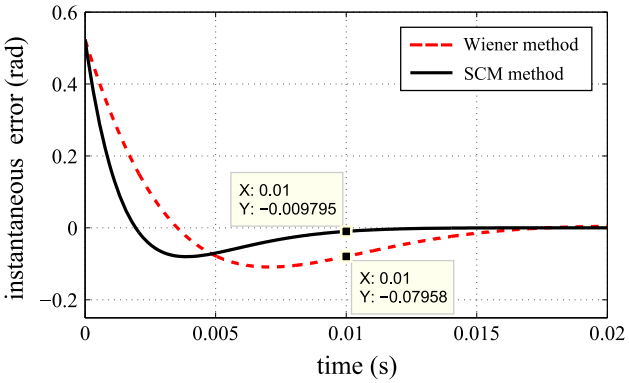

Fig. 4 Instantaneous phase error of the SRF PLL when subject to a $\pi/6$ rad phase jump, using Trial-1 Wiener method and the proposed SCM method of filter design (Error quantization) (Color figure online)

$0.009795 \times 2 \approx 0.02$ rad (since the error envelope encompasses the instantaneous error on both sides). The SCM method thus quantizes error with the required dynamic performance, while with the Wiener method, the error band is much higher (0.16 rad) than the specified limit at settling

time. The dynamic performance requirement is not met with Trial-1 Wiener method, and further iterations may still not yield optimum parameters.

It may be evident from Table 1 that the bandwidths in these two cases (Trial-1 Wiener v/s SCM) are not similar, and hence the comparison may appear to be unfair. It will soon be shown, however, that this selection of a nominal bandwidth for the Wiener method is reasonable. And though the Wiener method does not permit a large increase in bandwidth to improve dynamics lest filtering may be adversely affected, this time we choose a higher bandwidth for Trial-2 Wiener method. With the assumed parameters of $\delta = 0.707$ and $\omega_n = 598.32$ rad s^{-1} yielding a bandwidth which is similar to that computed by the SCM, the error band is nearly contained to the limits at the desired settling time, as is recorded under Trial-2 Wiener method in Table 1. However, to fulfil this dynamic requirement by Wiener technique, the filter parameters are more strained than those computed by the SCM, as is evident from the values of k_p, k_i and τ with the two methods. A relaxed time constant of 3.42 ms with the SCM method indicates the ease with which the filter may operate to meet the transient requirement, when compared to that of 2.36 ms with the Wiener method for the same transient requirement. This confirms that the SCM not only tunes the bandwidth to achieve the desired transient response, but also optimizes the filter parameters to achieve this with the least difficulty in practical filter implementation.

The concept of trade-off in Wiener optimization is appreciable in the case of stand-alone SRF PLL, due to the inability of SRF PLL in tracking an input affected with unbalance or harmonics. By having a nominal bandwidth setting, we obtain better rejection in the presence of polluted grids, while compromising a little on the transients. However, there is no reason for the enhanced SRF-based 3-phase PLLs to continue to use this trade-off as in the Wiener technique, when filtering is no longer a burden on the terminal SRF stage. And if they are to use this approach with increased bandwidths, it is visible that even with multiple tuning iterations, the Wiener optimization method may not guarantee the non existence of a better design, one which is directly achieved by the SCM, for the given error specifications.

Thus the SCM method plays an integral role in error quantization by optimally containing the transients in one run, which may not be possible even with rigorous trials of the Wiener optimization method.

3.2 Damping Optimization Using the SCM

To illustrate the importance of optimizing damping with the SCM, we perform further trials on the Wiener method, this time fixing the natural frequency at the optimum ($\omega_n = 531.71$ rad s^{-1} computed by the SCM), and selecting two values of δ, one lower ($\delta = 0.707$) and the other higher

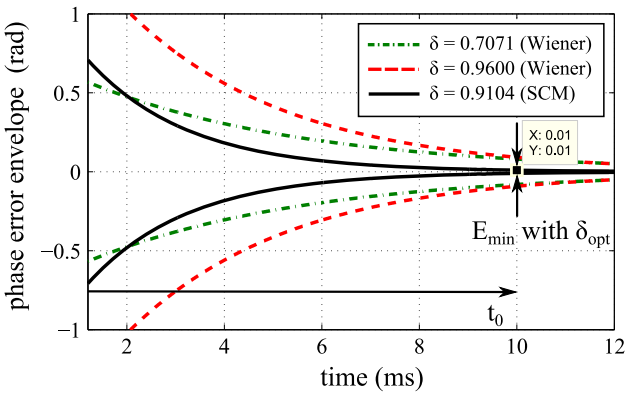

Fig. 5 Envelopes of phase tracking error of the SRF PLL when subject to a phase jump of $\pi/6$ rad, using Trial-3 and Trial-4 Wiener method and the proposed SCM method of filter design (Damping optimization) (Color figure online)

($\delta = 0.96$) than the optimum damping ratio ($\delta_{opt} = 0.91$ computed by the SCM). Note that selecting the optimum ω_n for the Wiener method is only for illustrative purpose. In reality, the optimum parameters cannot be speculated, and requires solving the SCM.

When subject to a phase jump of $\pi/6$ rad, the values of the error bands observed at settling time are recorded under Trial-3 and Trial-4 Wiener method in Table 1. It can be inferred that using non-optimum damping constants (both below and above δ_{opt}), the phase error band is always greater than that using the optimized damping factor. This is in coherence with the theory beneath the damping optimization equation, which yields the most optimum damping factor for the given values of natural frequency, worst-case frequency step and phase jump, such that the resulting error is always minimum at the settling time. Any other value of damping factor would result in larger error bands at the settling time.

The error envelopes corresponding to Trial-3 and Trial-4 Wiener approach are obtained and compared with that of the SCM method in Fig. 5. It is clearly visible that at the settling time, the least error band occurs with the SCM filter design, which optimizes damping for the given specifications.

Thus the remarkable importance of optimizing damping in the context of SCM based loop filter design is appreciable.

3.3 Performance Comparison When Subject to a Step Change in Frequency

Having computed the optimum filter design parameters for a phase jump previously, we now subject the SRF PLL to a step change in frequency. With the same error limits of 0.02 rad at 0.01 s, the SCM is rerun, this time to design for a worst-case frequency step of 10 Hz. The computed values of optimized parameters obtained by the SCM are recorded in Table 2.

Table 2 Filter design using the Wiener and the proposed SCM method, for a maximum error band of 0.02 rad at settling time 0.01 s, when the SRF PLL is subject to a frequency step of 10 Hz

Method	δ	ω_n (rad s^{-1})	k_p	k_i	τ (ms)	Bandwidth $2\delta\omega_n$ (rad s^{-1})	Error band observed at t_0 (rad)
Wiener	0.707	314.16	−1.37	−303.4	4.50	444.2	0.061
SCM	0.88	398.10	−2.16	−487.2	4.43	702.5	0.020

Henceforth, we choose nominal Wiener parameters as recorded in Table 2, for all comparisons between the Wiener and the SCM design methods, owing to the following reasons.

1. The Wiener method does not permit a large increase in bandwidth, in order to retain the trade-off between filtering and fast tracking
2. It is reasonable to select a nominal bandwidth, since this is a method that uses trial and error rather than a systematic approach
3. The optimum filter parameters are not known to the Wiener method as they are arrived at by solving the SCM
4. Even if the Wiener method was to select a similar bandwidth as the self-consistent computed bandwidth, it would result in non-optimum filter implementation, as shown earlier
5. Solving for a combination of frequency step and phase jump increases the complexity of the underlying equations manifold, which require an extensive analytical approach as in the SCM; even rigorous trials of Wiener method may not be successful in achieving the optimum filter design

The response of the SRF PLL to a step change in frequency can be compared for the two design methodologies by analysing the instantaneous phase error variation, as plotted in Fig. 6. It is observed that the phase error is confined to a narrower band and the SRF PLL settles faster using the optimized filter parameters computed by the SCM. And for the assumed parameters in the Wiener approach, it clearly requires further iterations to achieve the desired dynamic response, as error is not quantized at the required settling time with a nominal bandwidth setting.

3.4 Performance Comparison Under the Combined Effect of Frequency Step and Phase Jump

To be able to limit the tracking error for the case when both frequency excursion and phase jump occur, the design of the SCM is done assuming a worst-case combination of the two. While the specified error limit of 0.02 rad at 0.01 s is to be met for a combined maximum frequency step of 10 Hz and phase jump of $\pi/6$ rad, it is evident from Table 3 that the SCM guarantees the required transient response even for the worst-case, which is when they are of opposite polarities. For any better combination of instantaneous frequency step and phase jump, the error band at settling time is well within the limit specified. On the other hand, since the Wiener method does not account for frequency and phase fluctuations in filter optimization, it is observed that the error is not contained even for the best-case scenario, requiring tedious reattempts.

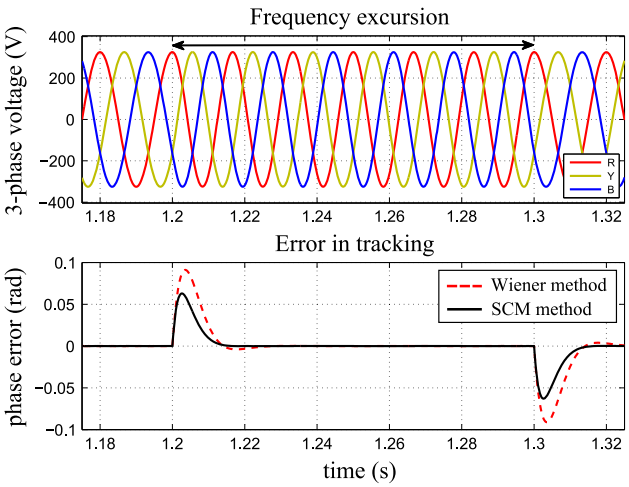

Fig. 6 Comparison of the phase error of SRF PLL when subject to a frequency step of 10 Hz, between the Wiener and the proposed SCM method of filter design (Color figure online)

3.5 Performance Comparison When Applied to the Improvised SRF-Based 3-Phase PLLs

Since the proposed SCM approach was originally aimed at the advanced SRF-based 3-phase PLLs, it is reasonable to assess the performance improvement when applied to the existing PLL structures from literature. For this purpose, we choose the DDSRF, DSOGI, and MCCF PLL, and compare their transient responses between the Wiener method and the SCM method of loop filter design.

These schemes are implemented in MATLAB/Simulink, and the simulated phase error is subjectively used to compare the dynamic performance and ease of filter design between

Table 3 Filter design using the Wiener and the proposed SCM method, for a maximum error band of 0.02 rad at settling time 0.01 s, when the SRF PLL is subject to a frequency step of 10 Hz and phase jump of $\pi/6$ rad

Method	δ	ω_n (rad s^{-1})	Combination	Instantaneous frequency step (Hz)	Instantaneous phase jump (rad)	Error band observed at t_0 (rad)
Wiener	0.707	314.16	Best-case	+10	$+\pi/6$	0.125
				−10	$-\pi/6$	
			Worst-case	+10	$-\pi/6$	0.209
				−10	$+\pi/6$	
SCM	0.911	551.86	Best-case	+10	$+\pi/6$	0.013
				−10	$-\pi/6$	
			Worst-case	+10	$-\pi/6$	0.020
				−10	$+\pi/6$	

the two methods. To appreciate the importance of decoupling between filtering characteristic and dynamic response with the improvised 3-phase PLLs, we also study the error transients under the effect of imperfections like voltage unbalance and harmonics. For the analyses, nominal Wiener parameters are chosen while the SCM computes the optimized parameters for the worst case frequency step and phase jump, as recorded in Table 3.

Figure 7a compares the instantaneous error between the Wiener method and the SCM method of filter optimization, when subject to a 10 Hz frequency excursion. As it is seen, all four PLL schemes are able to track frequency fluctuations (as is theoretically expected) but with different dynamics. The SRF PLL has a better response time among the four, while the DDSRF PLL has the least overshoot. However, a consistent improvement is seen in each of the four PLLs' response when the filter parameters of the terminal SRF stage are optimized using the SCM method.

Figure 7b compares the instantaneous error of the four PLLs when subject to a $\pi/6$ rad phase jump. In this case also, each of the four PLLs is able to track phase fluctuations in the input. The DDSRF PLL adjusts faster to the change, while the SRF PLL has the highest overshoot. However, between the Wiener and the SCM method, significant improvement is observed with the latter, without the need of multiple trials.

To simulate the response in the presence of unbalance and harmonics in the input, the grid simulator injects up to 10 % of unbalance and/or 5th, 7th, 11th and 13th order of harmonics in decreasing proportions. As is theoretically expected, the SRF PLL fails to track an input affected by voltage unbalance or harmonics. This is evident from the continued higher order oscillations in the phase error of the SRF PLL in Fig. 7c and d. However, with the augmented stages as in DDSRF, DSOGI, and MCCF PLL, the phase error settles even under voltage unbalance, as seen in Fig. 7c.

For the case when the input has higher order harmonics along with voltage unbalance, the MCCF PLL settles very quickly in comparison to the DDSRF or DSOGI PLL, which have small-scale oscillations in the phase error, as seen in Fig. 7d. The comparison of interest, however, is the dynamics of the tracked phase between the Wiener and SCM methods of filter design. As it is observed in the cases discussed so far, the profile of tracking error is significantly compacted, both along the 'x' (time) and 'y' (error) axes, using the SCM design method. This further highlights the importance of the self-consistent relationship between optimized damping and quantized error.

4 Conclusions

One of the key elements of this study is to advert to the plausible decoupling of the dependency between filtering and fast tracking, and hence eliminate any trade-off in tuning the PI filter parameters. The complexity in running two algorithms (error quantization and damping optimization) self-consistently in the backdrop is abstracted by a simple and minimal set of requirements from the designer. The other noteworthy contribution toward filter parameter selection is the technique to compute a distinguished pair of damping ratio (δ) and natural frequency (ω_n) for a defined error specification, thus ruling out the encumbrance of trial and error, and also yielding the best possible design. Theoretical basis beneath the derived mathematical expressions is strengthened by the inferences from the 3-D lookup tables. The key intent of this approach, which is to optimally improve the dynamic response of SRF-based 3-phase PLLs to grid fluctuations, is clearly met, as demonstrated by the results.

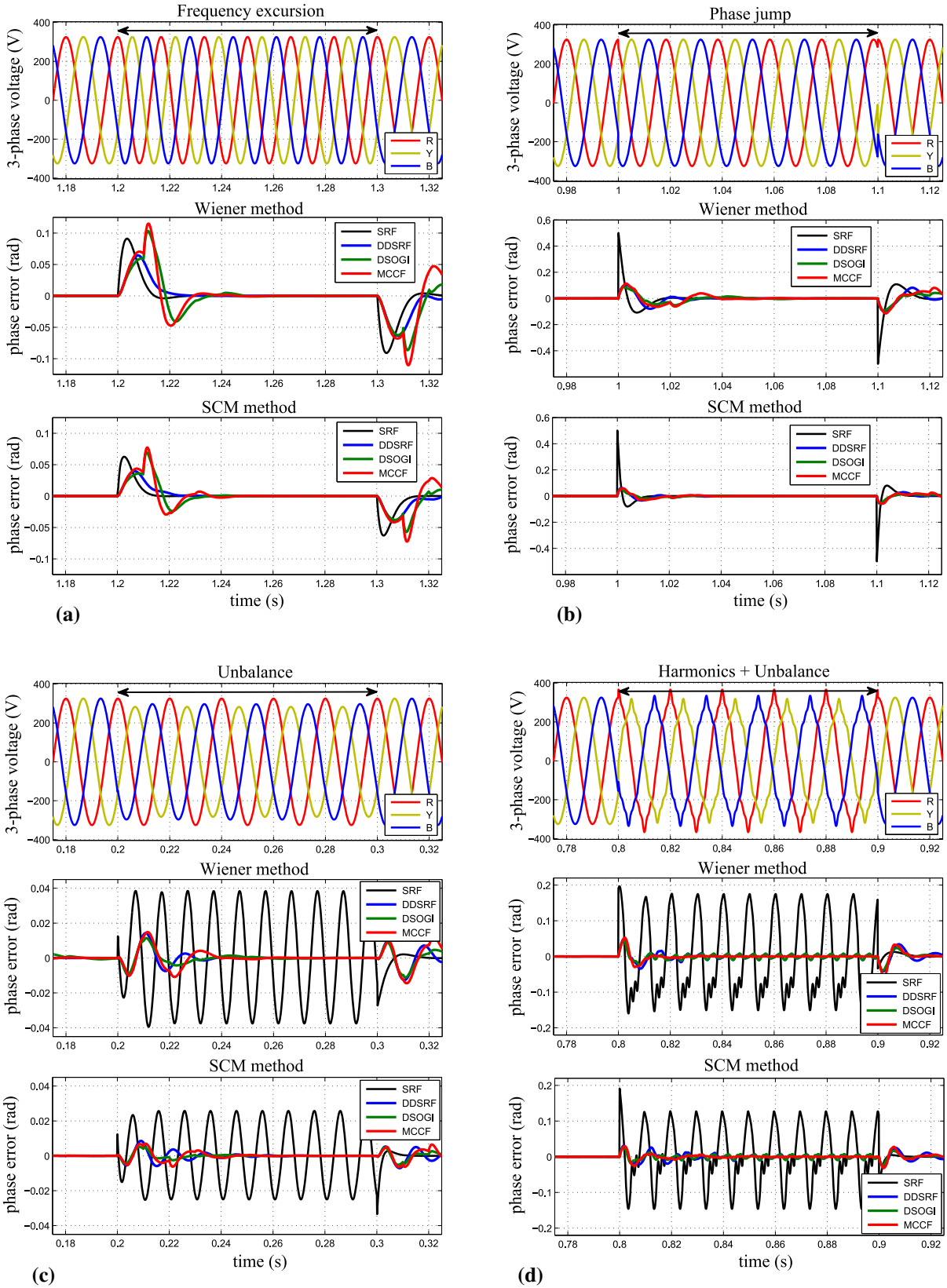

Fig. 7 Comparison of the phase error of SRF, DDSRF, DSOGI and MCCF PLL between the Wiener and the proposed SCM method of filter design **a** When subject to a frequency step of 10 Hz, **b** When subject to a phase jump of $\pi/6$ rad, **c** When subject to voltage unbalance (up to 10 %), **d** When subject to harmonics with voltage unbalance (Color figure online)

References

Chung, S. K. (2000). A phase tracking system for three phase utility interface inverters. *IEEE Transactions on Power Electronics*, *15*(3), 431–438.

da Silva, C. H., Pereira, R. R., da Silva, L. E. B., Lambert-Torres, G., Bose, B. K., & Ahn, S. U. (2010). A digital PLL scheme for three-phase system using modified synchronous reference frame. *IEEE Transactions on Industrial Electronics*, *57*(11), 3814–3821.

Gardner, F. M. (2005). *Phaselock techniques* (3rd ed.). New Jersey: John Wiley & Sons Inc.

Golestan, S., Monfared, M., Freijedo, F. D., & Guerrero, J. M. (2012). Design and tuning of a modified power-based PLL for single-phase grid-connected power conditioning systems. *IEEE Transactions on Power Electronics*, *27*(8), 3639–3650.

Guo, X., Wu, W., & Chen, Z. (2011). Multiple-complex coefficient-filter-based phase-locked loop and synchronization technique for three-phase grid-interfaced converters in distributed utility networks. *IEEE Transactions on Industrial Electronics*, *58*(4), 1194–1204.

Karimi-Ghartemani, M., & Iravani, M. R. (2004). A method for synchronization of power electronic converters in polluted and variable-frequency environments. *IEEE Transactions on Power Systems*, *19*(3), 1263–1270.

Kaura, V., & Blasko, V. (1997). Operation of a phase locked loop system under distorted utility conditions. *IEEE Transactions on Industry Applications*, *33*(1), 58–63.

Kulkarni, A., & John, V. (2013). Analysis of bandwidth—unit vector distortion trade off in PLL during abnormal grid conditions. *IEEE Transactions on Industrial Electronics*, *60*(12), 5820–5829.

Lee, K. J., Lee, J. P., Shin, D., Yoo, D. W., & Kim, H. J. (2014). A novel grid synchronization PLL method based on adaptive low-pass notch filter for grid-connected PCS. *IEEE Transactions on Industrial Electronics*, *61*(1), 292–301.

Liccardo, F., Marino, P., & Raimondo, G. (2011). Robust and fast three-phase PLL tracking system. *IEEE Transactions on Industrial Electronics*, *58*(1), 221–231.

Rodríguez, P., Teodorescu, R., Candela, I., Timbus, A., Liserre, M., Blaabjerg, F. (2006). New positive-sequence voltage detector for grid synchronization of power converters under faulty grid conditions. In: Proc. 37th IEEE PESC, pp 1–7.

Rodríguez, P., Pou, J., Bergas, J., Candela, J. I., Burgos, R. P., & Boroyevich, D. (2007). Decoupled double synchronous reference frame PLL for power converters control. *IEEE Transactions on Power Electronics*, *22*(2), 584–592.